Published in final edited form as:
Acta Biomater. 2009 June ; 5(5): 1389–1398. doi:10.1016/j.actbio.2008.11.003.

Superhydrophobic Effect on the Adsorption of Human Serum Albumin

Evan S. Leibner[•], **Naris Barnthip**[†], **Weinan Chen**[•], **Craig R. Baumrucker**[°], **John V. Badding**[•,‡], **Michael Pishko**[◆], and **Erwin A. Vogler**[*,†,‡]

[†]Department of Materials Science and Engineering, The Pennsylvania State University University Park, PA 16802

[‡]Department of Bioengineering, The Pennsylvania State University University Park, PA 16802

[°]Department of Dairy and Animal Science, The Pennsylvania State University University Park, PA 16802

[•]Department of Chemistry The Pennsylvania State University University Park, PA 16802

[*]Huck Institute of Life Sciences and Materials Research Institute The Pennsylvania State University University Park, PA 16802

[◆]Department of Chemical Engineering, Texas A&M University, College Station, TX 77843

Abstract

Analytical protocol greatly influences measurement of human-serum albumin (HSA) adsorption to commercial expanded polytetrafluororethylene (ePTFE) exhibiting superhydrophobic wetting properties. Degassing of buffer solutions and evacuation of ePTFE adsorbent to remove trapped air immediately prior to contact with protein solutions are shown to be essential. Results obtained with ePTFE as a prototypical superhydrophobic test material suggest that vacuum degassing should be applied in the measurement of protein adsorption to any surface exhibiting superhydrophobicity. Solution depletion quantified using radiometry (I-125 labeled HSA) or electrophoresis yield different measures of adsorption, with nearly four-fold higher surface concentrations of unlabeled HSA measured by the electrophoresis method. This outcome is attributed to the influence of the radiolabel on HSA hydrophilicity which decreases radiolabeled-HSA affinity for a hydrophobic adsorbent in comparison to unlabeled HSA. These results indicate that radiometry underestimates the actual amount of protein adsorbed to a particular material. Removal of radiolabeled HSA adsorbed to ePTFE by 3X serial buffer rinses also shows that the remaining “bound fraction” was about 35% lower than the amount measured by radiometric depletion. This observation implies that measurement of protein bound after surface rinsing significantly underestimates the actual amount of protein concentrated by adsorption into the surface region of a protein-contacting material.

Keywords

Protein adsorption; interphase; surface; radiometry; depletion

1.0 Introduction

Surface engineering has had a long and successful role in the development of biomaterials for a wide variety of medical devices to improve compatibility with blood and tissue.[1-14] A

*Author to whom correspondence should be addressed Erwin A. Vogler EAV3@PSU.EDU Phone (814) 863-7403 Fax (814) 865-2917.

recent trend in surface engineering has been texturing surfaces at the micro-to-nanoscale to influence important interfacial events such as protein adsorption[15,16] and cell adhesion.[17,18] A particular subgroup of textured materials of interest to this work are poorly-water-wettable (hydrophobic) materials exhibiting “superhydrophobicity” or ultra-high water repellency[19-29] (also occasionally termed ultrahydrophobic[19,22] and super anti-wetting [23] in the literature). The superhydrophobic effect ultimately arises from air trapped within the interstices of a rugose surface (patterned or random) that water fails to wet or wick into, so that water is partially riding on a cushion of air, yielding observed water contact angles much greater than the inherent contact angle of the smooth material; sometimes in excess of 150°. The superhydrophobic effect is common in nature, accounting for the water-repellent properties of bird feathers and plant leaves (the “Lotus Effect”)[21,22,30-32] as examples. Certain materials in widespread biomedical application such as expanded polytetrafluororethylene (ePTFE) are superhydrophobic as commercially prepared because of the inherent hydrophobicity of PTFE (advancing water contact angle of about 114 °)[33] and a fibrillated texture introduced by biaxial stretching (see Figure 1.).[34,35] For example, we observe an advancing contact angle of about 138° on the ePTFE used in this work. The blood compatibility of ePTFE vascular grafts[36,37] has stimulated interest in understanding, and improving upon, biocompatibility of the general class of superhydrophobic materials.

A fundamental aspect of biocompatibility is protein adsorption.[38-43] Consequentially, protein adsorption to superhydrophobic materials is important to fully characterize. The general literature on protein adsorption is controversial and inconsistent[44,45], and so it should be of no particular surprise that there is considerable diversity of opinion regarding protein-adsorption properties of superhydrophobic materials, with some investigators reporting protein-adsorbent properties[16,36] and others non-adsorbent properties.[26,32,46]

We have initiated a program investigating a novel jet-blowing method of producing nano-fibrous PTFE for biomedical applications[47,48] and have interest in relating protein adsorption to material properties and processing conditions, using commercial ePTFE (Figure 1) as a reference material. Herein, we report that analytical protocol greatly affects measurement of human serum albumin (HSA) to ePTFE and show that different methods of calculating amount adsorbed (bound vs. solution depletion) give rise to quite different impressions of ePTFE adsorbent capacity.

2. Methods and Materials

2.1 Protein Solutions

Fraction V HSA (MW = 66.3 kDa, 96-99%, lyophilized powder) was used as received from Sigma Aldrich (St. Louis, MO) with no further purification. Solutions were prepared in phosphate buffer saline PBS (0.01 M PBS, prepared in 18 mΩ water) degassed under reduced pressure obtained by evacuating the headspace with a rotary vacuum pump (approximately 500 torr) for 5 minutes. HSA was labeled using the Chloramine T method [49-51] for 30 seconds to yield specific activity of 36.4 μCi/μg. We estimated that an average of ~3 iodine molecules were incorporated into each molecule of HSA (see Appendix A). HSA radioactivity (counts-per-min, CPM) was measured by gamma counting in a Wallac 1470 Wizard Automatic Gamma Counter (PerkinElmer). Free Iodine was separated from the labeled protein using a G 50 sephadex column (Sigma Aldrich, St. Louis, MO). Labeled protein was stored at 2°C and used within 2 weeks, over which time protein degradation was regularly assessed by chromatography on a G 100 sephadex column (Sigma Aldrich St. Louis, MO) to detect protein fragments or aggregation. Analysis of chromatographic peak area revealed that less than 10% of labeled protein was affected by radiolysis over the 2 week storage period. Test protein solutions were prepared by mixing 3 μL of stock labeled protein solution with 1.5 mL

unlabelled protein solution at the desired concentration to yield approximately 0.09 μCi in each 200 μL sample.

2.2 ePTFE Adsorbent Preparation

Expanded ePTFE was a gift from Atrium Medical Corp (Hudson, NH). As illustrated in the left-hand side of Figure 2, 20 mg portions were weighed into glass screw-top glass vials VWR (West Chester, PA) using a precision microbalance XS 105, Mettler Toledo. Each vial was fitted with a rubber septum lined with PTFE with an evacuation port. Air was continuously evacuated from the vial through a syringe needle connected to a rotary vacuum pump (Precision, 1/8 HP) during subsequent wetting steps in which ePTFE was first pre-wet with 1 mL of 100% ethanol (EtOH, Pharmco) followed by 3X serial rinsing with 1 mL of degassed PBS. The vacuum pump was double trapped to assure no backflow into the vial. Just before the vacuum line was removed, 200 μl of test HSA solution injected onto through the septum to completely cover ePTFE adsorbent using a precision volumetric syringe (700 Series Hamilton, 250 μl) fitted with a Chaney adapter that assured reproducible volumetrics.

Surface area of the ePTFE used in this work was measured using the BET method on the Micromeritics ASAP 2000 using nitrogen as the probe gas. SEM images shown in Figure 1 were obtained on the JEOL 6700F field emission scanning electron microscope. ePTFE samples were mounted on SEM stubs with small amounts of conductive tape and sputter coated with Iridium. No attempt was made to further interpret surface area measurements in terms of porosity or size of putative pores.

2.3 Protein-Adsorption Methods

Figure 2 further outlines general aspects of the protocol used to construct HSA adsorption isotherms. Radiometry was implemented two ways: (1a) radiometric measurement of solution depletion (counts remaining in solution after contact with ePTFE) for direct comparison with the electrophoresis method 2 (see further below) and (1b) measurement of “bound” HSA (counts remaining after 3X serial wash of ePTFE) for comparison of bound HSA to solution depletion. Radiometric HSA adsorption isotherms were constructed by measuring the amount of I-125 labeled HSA adsorbed to ePTFE (see further below) from bulk-solution concentrations $0 \leq W_B^o \leq 50$ mg/mL prepared in 5 mg/mL increments using degassed PBS. 3 μl of hot trace of I-125 labeled HSA was mixed into 1.5 mL HSA solution at each concentration. Measurements at each HSA concentration were made in triplicate using 3 separate samples of ePTFE and carrying 3 empty vials as blanks. Labeled HSA solutions were equilibrated with ePTFE for 1 hour during which time total radioactivity was integrated using on the gamma counter. 200 μl of HSA solution was aspirated from the test vial using a pipette and transferred into a (VWR, 12 × 75mm) test tube. The pipette transfer tip (VWR 1-200 μl Barrier Tips) was placed into the test tube along with solution to eliminate possibility of protein loss. ePTFE remaining in the original vial was serially rinsed 3X with 200 μl of degassed PBS, collecting wash and tip into separate test tubes (with the tip) for each wash (see Figure 2). Mass balance was found to be with ± 5 % of the radioactivity in the starting solution, verifying no significant protein loss through the protocol. Depletion was corrected for background by subtraction of the average background determined from the triplicate blank vials. Triplicates were averaged and standard deviation of the mean accepted as an adequate measure of experimental error. Appendix B details of the calculations used in radiometry.

Adsorption kinetics were not measured in this work and 1 hour equilibration time was assumed to be sufficient to reach adsorption steady state based on prior kinetics measurements using interfacial energetics.[43,52-58] Indeed, recent studies of protein adsorption kinetics reveal that mass adsorption rates significantly exceed rate-of-change in interfacial energetics due to

adsorption [59], leading us to conclude that 1 hour adsorption equilibration time was conservative by at least 10 fold.

2.4 Protein-Adsorption by Electrophoresis

The lower-right-hand panel of Figure 2 outlines basic steps used in the electrophoretic implementation of the standard solution-depletion measurement of unlabeled HSA adsorption (see refs.[60-63] for experimental details and example applications). Briefly, for the purpose of this report, HSA adsorption isotherms measured by depletion using bulk-solution concentrations $0 \leq W_B^o \leq 50$ mg/mL prepared in 5 mg/mL increments in degassed PBS. Sample preparation was as described in section 2.2 above. Electrophoresis was performed using 26 lane NuPAGE® Novex Tris-Acetate precast gels (Invitrogen; 500 kDa capacity) carried out for 1 hour at 150 V using an XCell SureLock™ Cell (Invitrogen). Gels were stained with SimplyBlue™ SafeStain (Invitrogen) for 1 hour and destained with de-ionized (18 MΩ) water for several hours while mixing on a standard hematology rocker. Band intensity was quantified using the Gel-doc system (Bio-Rad Laboratories) that employed a highly-sensitive CCD camera to read optical density (OD). A standard curve was prepared for each gel using the first 6-7 lanes by applying solutions of known (by gravimetry) HSA concentrations. Linear calibration curves were obtained (R^2 > 98%) within the concentration range 1 to 50 mg/mL for all gels used in this work. Previous work has "certified" this method of measuring protein adsorption by first studying adsorption of a broad range of single proteins to hydrophobic [60] surfaces (octyl sepharose and silanized glass) from aqueous-buffer solution, showing that results comported with thermochemically-measured free energies of adsorption and interfacial energetics measured by tensiometry (contact angle and wettability methods). Subsequently, HSA adsorption to silanized-glass adsorbent particles with incrementally-increasing hydrophilicity was measured,[61] showing here that mass and energy balances for HSA adsorption were in full agreement. Consistent mass-and-energy balance obtained using very different analytical methods engendered confidence that this gel-electrophoresis implementation of the depletion method provided internally-consistent and accurate results; at least for proteins adsorbing to surfaces from stagnant fluids at steady state. It is important to emphasize that previous work has shown that periodic or continuous mixing (by agitating tube contents or using a hematology rocker, respectively) does not influence results.[60] Furthermore, time-and-concentration interfacial energetics of a wide variety of blood proteins and mixtures shows that adsorption to stagnant buffer/air or buffer/solid surfaces comes to steady state within the 1 hour equilibration time utilized in depletion experiments.[43,52-58, 64]

3. Results

3.1 ePTFE Adsorbent

BET surface area measurements and electron microscopy show that ePTFE used in this work was of very high specific surface area (5.57 ± 0.09 m^2/gram) due to the fibular structure that is a product of biaxial stretching. Close examination of these fibers (Figure 1) indicates numerous cracks, fissures, and spaces that confer a high degree of porosity. No attempt was made by this work to further analyze surface area in terms of porosity or measure the size distribution of pores relative to molecular dimensions of HSA (3.6 nm hydrodynamic radius [52,65]). However, it is visually evident from Figure 1 that many of the cracks, fissures, and spaces are much larger than HSA itself, most probably accounting for the high absorbency reported in the following sections that exceeds the 2-3 mg/m^2 typically anticipated for protein adsorption to smooth surfaces by 10 fold or more (see Table 1). Without detailed porosity information, it is not possible to fully account for measured adsorbed mass (as measured by the 3 methods discussed below) in terms of the geometry of adsorbed HSA or possible formation of adsorbed multilayers.

3.2 Comparison of Experimental Protocols

Figure 2 depicts general aspects of the experimental protocol applied in this work to measure HSA adsorption to ePTFE (see also Section 2). PBS solutions containing initial HSA concentrations $0 \leq W_B^o \leq 50$ mg/mL were brought into contact with 20 mg of ePTFE either under ambient conditions or under vacuum to remove air (left-hand side of Figure 2). After 1 hour equilibration, protein solution was separated from the ePTFE by aspiration (right-hand side of Figure 2). Adsorbed protein was measured one of two ways: (1) radiometry for I-125 labeled HSA (upper quadrant, right-hand side of Figure 2)[66-73] or (2) solution depletion implemented using electrophoresis for unlabeled HSA (lower quadrant, right-hand side of Figure 2).[60-63] Radiometry was itself implemented two ways: (1a) radiometric measurement of solution depletion (counts remaining in solution after contact with ePTFE) for direct comparison with method (2) and (1b) measurement of "bound" HSA (counts remaining after 3X serial wash of ePTFE) for comparison of bound HSA to solution depletion.

Figure 3 compares radiometric measurement of surface-bound HSA (open circles) to the amount depleted from solution depletion (open diamonds) obtained by either bringing protein solutions into contact with ePTFE under vacuum (Panel A) or under ambient conditions (Panel B). Comparison of Panel A with Panel B clearly reveals that removal of air from the surface was essential to measuring HSA adsorption to ePTFE at any solution concentration. Comparison of different experimental strategies optionally combining solution degassing with evacuation revealed that reliable results could be obtained only when HSA solutions prepared in degassed PBS were brought into contact with ePTFE under vacuum. If either of these two steps were not applied, results were erratic; sometimes leading to measurable adsorption and sometimes not (not shown). If neither PBS degassing nor evacuation were used, typically no adsorption was measurable, except for an occasional spurious adsorption event at higher-solution concentrations (Figure 3B).

3.3 Adsorption Isotherms of I-125 Labeled HSA

Data of Figure 3A constitute adsorption isotherms comparing "total" radiolabeled HSA adsorbed (by solution depletion) and "bound" HSA (remaining on ePTFE after 3X rinsing). Both radiometric methods revealed that the amount of HSA adsorbed increased in proportion to solution concentration, up to an apparent surface saturation that occurred at a statistically-identical solution concentration $\left(W_B^o\right)^{\max}$ (mg/mL; see Table 1 and Figure 3A annotations). Lines drawn through the data of Figure 3A (best fit lines through the linear regions) nominally suggest that the total amount of HSA adsorbed was greater than bound HSA at any $W_B^o \geq 10$ mg/mL. Table 1 compares quantitative parameters derived from statistical treatment of data of Figure 2A (see Section 2) under the heading "Radiometry", where $\Gamma^{\max}$ measured maximum bound HSA and $D^{\max}$ maximum total adsorbed (see Figure 3A annotations). Note that $D^{\max}$ in Table 1 is expressed both in terms of surface concentration mg/m^2 and mg/mL bulk solution (maximal solution depletion). Slopes S of total and bound adsorption isotherms were statistically different at the 1σ (65%) confidence interval (Table 1) but not at 2σ (95%) confidence.

Figure 4 shows the distribution of radioactivity among total (depletion), bound, and 3X serial rinses for one of triplicate radiometric adsorption experiments performed at $0 \leq W_B^o \leq 30$ mg/mL solution concentrations. Inspection reveals that third-rinse solutions contained little radioactivity. We thus concluded that additional PBS rinsing would have little impact on the measured bound fraction and, further, that the bound fraction was between 38.5% to 50.8 % (corresponding to 10 and 30 mg/mL solution concentration, respectively) of the total for these particular experiments. However, experimental error represented by 1σ error bars of Figure 3A (standard deviation of triplicates, see Section 2) clearly showed considerable variation

among triplicates, even though > 95% mass balance was obtained for each experiment involved in the triplicate trial (no loss of radioactivity). We thus concluded that an uncontrolled variable was responsible for experimental irreproducibility but that experimental precision was adequate to support the conclusions drawn in this paper.

3.4 Adsorption Isotherms of Unlabelled HSA

Figure 5 is an HSA adsorption isotherm for unlabelled HSA adsorption to ePTFE measured by the electrophoresis method (see Section 2), where the amount adsorbed was measured by the decrease in (depletion of) solution concentration (*D*, mg/mL) caused by contact with adsorbent, consistent with previous reports by this group.[60-63] This isotherm followed the same general trends obtained by radiometry (Figure 3A), except that the curve slope *S* was approximately 5X greater than obtained by radiometry (on a consistent mg/m^2 basis; compare row 3 column 4 Table 1 under the heading “Radiometry” to row 5 column 4 under “Electrophoresis”). Moreover, the estimated solution depletion at surface saturation $D^{\max}$ obtained by electrophoresis was about 4X greater than that obtained by radiometry (on a consistent mg/m^2 basis; compare row 3 column 2 Table 1 under the heading “Radiometry” to row 5 column 2 under “Electrophoresis”). Interestingly, the solution concentrations corresponding to surface saturation ($\left(W_B^o\right)^{\max}$ obtained by electrophoresis and radiometry were not statistically different (on a consistent mg/mL basis; compare entries in column 5 of Table 1 under “Radiometry” and “Electrophoresis” headings; see also Figure 3A).

4. Discussion

4.1 Effect of Trapped Air in Superhydrophobic Materials

Comparison of results obtained by experimental protocols outlined in Figure 2 shows that elimination of air from ePTFE adsorbent and degassing of solutions is essential to obtaining reliable measures of HSA adsorption. Significant HSA adsorption was measured if evacuation and degassing steps were included in the protocol (Figure 3A) whereas no adsorption was measured under ambient conditions (Figure 3B). Erratic results were obtained when either of these steps were not used (not shown). We attribute this outcome to the variable presence of air trapped within the interstices of the fibular ePTFE structure that prevented intimate contact with HSA solutions with the solid phase. Given that trapped air gives rise to superhydrophobic wetting properties, we speculate that the evacuation/degassing protocol is a necessary step for reliable measurement of protein adsorption to any superhydrophobic material. We further speculate that the erratic results obtained when evacuation/degassing is not rigorously followed accounts for conflicting literature reports of protein adsorption to materials exhibiting superhydrophobic wetting properties.

4.2 Radiometric Assessment of Solution Depletion and Bound Protein

Solution depletion is a venerable method of measuring the total amount of protein adsorbed to a material immersed in a protein solution. This mass-balance method is, for the most part, unambiguous because no surface-rinsing steps are involved that might perturb the “interphase” region separating the physical surface from the bulk solution or lead to artifacts related to drying between rinses.[60-63] However, solution depletion does not resolve adsorbed protein into strongly-and-loosely adsorbed fractions, reporting only the total amount removed from the solution phase by contact with adsorbent. Rinsing is frequently applied to eliminate contribution from the bulk solution, assuming that only the bound fraction that resists rinsing from the surface is important and that the loosely-adsorbed fraction is either irrelevant or negligible. Figs. 3A and 4 together show that rinsing does remove a significant portion of adsorbed protein and that the bound fraction is, in fact, only between 30 and 50% of the total ascertained by radiometric depletion, depending on solution concentrations employed. This

work does not attempt to measure the activity or biological importance of bound HSA in comparison that fraction that can be rinsed from the surface, but it is clear that this loosely-adsorbed fraction is certainly not negligible in quantitative terms. Thus, although rinsing is commonly applied in measurement of protein adsorption, especially in radiometric assays, accurate assessment and interpretation of adsorption must take into account both adsorbed fractions. Caution is especially warranted when two-or-more proteins are involved in adsorption competition to the same surface because it is not known how rinsing might affect the relative amounts of bound protein. We speculate that failure to account for total and bound fractions is a significant contributor to the notorious controversy that surrounds mechanistic studies of protein adsorption, and certainly a factor that complicates inter-comparison of results from different measures of protein adsorption (see ref. [44] and citations therein). Furthermore, the fact that the substantial portion of HSA adsorbed to ePTFE can be rinsed from the adsorbent shows that protein adsorption is not inherently irreversible as proposed by different theories, such as the Random Sequential Adsorption (RSA) model (see refs. [58,61] and citations therein). Future work may well prove that the bound fraction is practically irreversible, but the majority of adsorbed HSA is easily displaced from ePTFE.

4.3 Effect of Radiolabeling

Covalent attachment of 3-4 iodine atoms per HSA molecule (see Appendix A) certainly affects protein structure and hydrophilicity to some extent.[70, 74-79] For examples, Desbuquois and Aurbach [75] showed that incorporation of more than one iodine atom per insulin molecule caused a significant change in protein solubility and Hunter *et al* [79] suggested that lysozyme hydrophilicity was affected by radiolabeling. However, in spite of persistent reports of radiolabeling artifacts, such effects are typically construed to be negligible for large proteins or simply ignored altogether, and radiometry has hence enjoyed widespread application in the measurement of protein adsorption. Comparison of results obtained by radiometric and electrophoretic depletion methods (Figure 3A and 5, respectively; see also Table 1) shows that I-125 radiolabeling of HSA reduces adsorption by nearly four fold. Labeled and un-labeled HSA adsorption isotherms were qualitatively similar in that each were adequately described by a simple Henry isotherm (adsorbed amount increases in direct proportion to bulk-solution concentration), corroborating previously published work from this group measuring adsorption of diverse proteins to surfaces spanning the full range of observable water wettability.[60-63] But lower adsorption of radiolabeled HSA to the same ePTFE adsorbent under identical conditions strongly suggest that significantly altered adsorption characteristics. Given that isotherm slopes *S* that measure protein-adsorption affinity were also sevenfold higher for unlabelled HSA (Table 1, leading to nearly four-fold difference in absolute amounts adsorbed), it is evident that the difference between radiometric (labeled) and electrophoretic (unlabeled) depletion assays increases linearly with solution concentration up to surface saturation. Thus, the discrepancy between adsorption measurements of labeled an unlabelled protein increases with solution concentration. Interestingly, however, the solution concentration corresponding to surface saturation ($\left(W_B^o\right)^{\max}$ was not statistically different for the different analytical protocols employed herein (see annotations on Figure 3A and Table 1). We interpret this latter observation to mean that presence of a few tracer molecules among an overwhelming number of unlabelled proteins did not measurably affect protein packing at the ePTFE surface that leads to surface saturation (more specifically stated, protein packing within the interphase region separating the physical ePTFE surface from bulk solution was not affected by the presence of a minority of tracer molecules). Apparently, a fixed proportion of the protein adsorbed within this interphase actually contacts the physical surface and engages in protein-surface interactions with sufficient strength to resist 3X PBS rinses. Based on data of Fig 3A. and section 3.2, we estimate that between 38.5% to 50.8% of adsorbed molecules actually contact the surface and become bound.

Thus, although radiometry has been widely applied in measurement of protein adsorption, the effect of the radiolabel on quantitation has apparently been under estimated, at least as measured here for HSA adsorption to ePTFE. The systematic effect of solution concentration on the measured difference between labeled and unlabelled results is of particular concern since this introduces yet another factor that complicates comparison of experiment from different laboratories. We speculate that failure to account for labeling artifacts is yet another significant contributor to the notorious controversy that surrounds mechanistic studies of protein adsorption.

5. Conclusions

Analytical protocol greatly affects measurement of human-serum albumin (HSA) adsorption to commercial expanded polytetrafluororethylene (ePTFE). Specifically, it was found that consistent adsorption results could be obtained only when ePTFE adsorbent was brought into contact with degassed protein solutions under vacuum (reduced air pressure). These observations strongly suggest that air trapped within the interstices of the fibular ePTFE structure that gives rise to superhydrophobic wetting properties prevents intimate contact with HSA solutions which, in turn, strongly influences protein-adsorption outcomes. Given that trapped air is the underlying cause of the superhydrophobic effect, results obtained with ePTFE imply that the trapped-air effect on protein adsorption is general and that removal of trapped air is essential to measuring protein adsorption to any material exhibiting superhydrophobicity.

Comparison of two methods of measuring adsorption, standard radiometry and solution depletion of unlabelled protein, showed that I-125 radiolabeling reduced the amount of HSA adsorbed to ePTFE by about four fold. Furthermore, the amount of bound HSA (that portion remaining on the adsorbent after 3X buffer rinsing) was found to be systematically lower than the total adsorbed from solution (quantified by solution depletion) and varied as a function of initial HSA solution concentration, up-toand-including surface saturation. Thus, I-125 radiolabeling of HSA appears to significantly alter protein adsorption properties and measurement of bound protein significantly underestimates the total protein actually adsorbed from solution.

Acknowledgements

We gratefully acknowledge Atrium Medical Corporation for the gift of ePTFE used in this work. This work was supported, in part, by the National Institute of Health grant R21 EB006093. Additional support for EV by the American Chemical Society Petroleum Research Fund grant #44523-AC5 and the National Institute of Health grants PHS 2R01HL069965 is also gratefully acknowledged. The Authors appreciate support from the Materials Research Institute, Departments of Materials Science and Engineering, and the Department of Chemistry, Penn State University.

Appendix

Appendix A: Estimate of Iodine Incorporation

Artifacts associated with radiolabeling presumable increase with the number of Iodine atoms incorporated per protein molecule, (see section 4.3). We estimate incorporation of 3 atoms of Iodine 125 per HSA molecule used in this work in the following way. 25 μg of HSA (2.26×10^{20} molecules at MW= 66.5KDa) was iodinated with 1mCi of Iodine 125 (6.53×10^{20}atoms, MW =53 g/mol) at a specific activity of 17.4 Ci/mg resulting in a solution of HSA with a specific activity of 36.4 μCi/μg. Trichloroacetic acid precipitation showed that that 93% of the 125I was attached to HSA, implying $\frac{6.07\times10^{20}\text{atoms I125}}{2.26\times10^{20}\text{molecules of HSA}}=2.7\,\frac{^{125}\text{I}}{\text{HSA}}$ or about 3 iodine atoms per HSA. This suggests that of the 19 tyrosine residues on each HSA molecule [80], of which 12 are on the solvent-exposed surface of the molecule and easily attacked [76], there is an average of 0.2 iodine atoms per surface tyrosine.

Appendix B: Radiometry

The basic idea behind the depletion method is to measure the amount of protein in solution before and after contact with adsorbent. If C_T is the counts/min (CPM) of the originating solution and C_L is CPM of the solution separated from adsorbent (see Figure 5), then depletion is $\Delta C = (C_T - C_R)$ CPM and the total mass of protein remaining in solution is $m_R = \left(\frac{C_R \times m_T}{C_T}\right)$ (mg); where m_T the total mass (mg) of protein in solution. Mass depletion is then $\Delta m = m_T - m_R$. Background is assumed to be the radioactivity depleted out of solution on to an empty glass vial controls (no ePTFE) m_D^b (mg). Thus the background corrected depletion $D = \Delta m - m_D^b$ (mg), normalized to surface area of the ePTFE S_a (m^2) or volume of the protein solution V (mL) is given by:

$$D = \frac{m_T - \left(\frac{C_L * m_T}{C_T}\right) - m_D^b}{S_a} \left(\mathrm{mg/m^2}\right)$$
or
$$D = \frac{m_T - \left(\frac{C_L * m_T}{C_T}\right) - m_D^b}{V} (\mathrm{mg/mL}) \quad (1)$$

Bound protein is the amount of protein that is remaining on the ePTFE surface after coming in contact with the protein solution and 3X PBS rinses (see Figure 5). If C_T is the counts/min (CPM) of the originating solution and C_A is CPM of the ePTFE surface after being separated from adsorbent, then the total mass of protein remaining on the surface is $m_A = \left(\frac{C_A \times m_T}{C_T}\right)$ (mg), where m_T is the total mass (mg) of protein in solution. Background is assumed to be the radioactivity remaining on an empty glass vial controls (no ePTFE) m_A^b (mg). Thus the background corrected adsorption $\left(m_A - m_A^b\right)$ (mg), normalized to surface area of the ePTFE S_a (m^2 or volume of the protein solution V (mL) is then:

$$\Gamma = \frac{\left(\frac{C_S \times P_T}{C_T}\right) - P_T^b}{S_a} \left(\mathrm{mg/m^2}\right)$$
or
$$\Gamma = \frac{\left(\frac{C_S \times P_T}{C_T}\right) - P_T^b}{V} (\mathrm{mg/mL}) \quad (2)$$

References

[1]. Williams, DF.; Bagnall, RD. Fundamental Aspects of Biocompatibility. CRC Press; Boca Raton: 1981.

[2]. Kim SW, Feijen J. Surface Modification for Improved Blood Compatibility. Critical Reviews in Biocompatibility 1985;1(3):229–61.

[3]. Cazenave, JP.; Davies, JA.; Kazatchine, MD.; Aken, WGv. Blood-Surface Interactions. Elsevier; Amsterdam: 1986. Blood Coagulation and Fibrinolysis; p. 153-61.

[4]. Elbert DL, Hubbell JA. Surface Treatments of Polymers for Biocompatibility. Annual Review Material Science 1996;26:365–94.

[5]. Horbett, TA.; Klumb, LA. Cell Culturing: Surface Aspects and Considerations. In: Brash, JL.; Wojciechowski, PW., editors. Interfacial Phenomena and Bioproducts. Marcel Dekker; New York: 1996. p. 351-445.

[6]. Vogler, EA. Interfacial Chemistry in Biomaterials Science. In: Berg, J., editor. Wettability. Marcel Dekker; New York: 1993. p. 184-250.

[7]. Miller R, Guo Z, Vogler EA, Siedlecki CA. Plasma Coagulation Response to Surfaces with Nanoscale Heterogeneity. Biomaterials 2006;27:208–15. [PubMed: 16011849]

[8]. Boyan B, Hummert T, Dean D, Schwartz Z. Role of material surfaces in regulating bone and cartilage cell reponse. Biomaterials 1996;17:137–46. [PubMed: 8624390]

[9]. Choi YJ, Choung SK, Hong CM, Shin IS, Park SN, Hong SH, et al. Evaluations of blood compatibility via protein adsorption treatment of the vascular scaffold surfaces fabricated with polylactide and surface-modified expanded polytetrafluoroethylene for tissue engineering applications. J Biomed Mater Res Part A Dec;2005 75A(4):824–31.

[10]. Hoffman, AS.; Ratner, BD. Nonfouling Surfaces. In: Ratner, B.; Hoffman, A., editors. Biomaterials Science: An Introduction to Materials in Medicine. Vol. 2 ed.. Elsevier Academic Press; San Diego: 2004.

[11]. Jozefonvicz J. Blood-Contacting Polymers. Polymeric Biomaterials 1994:349–71.

[12]. Peppas NA, Langer R. New challenges in biomaterials. Science Mar 25;1994 263(5154):1715–20. [PubMed: 8134835]

[13]. Tamada Y, Ikada Y. Effect Of Preadsorbed Proteins On Cell-Adhesion To Polymer Surfaces. J Colloid Interface Sci Feb;1993 155(2):334–9.

[14]. Xue L, Greisler HP. Biomaterials in the development and future of vascular grafts. J Vasc Surg Feb; 2003 37(2):472–80. [PubMed: 12563226]

[15]. Rechendorff K, Hovgaard MB, Foss M, Zhdanov VP, Besenbacher F. Enhancement of Protein Adsorption Induced by Surface Roughness. Langmuir. November 15;2006 2006

[16]. Zimmermann J, Rabe M, Verdes D, Seeger S. Functionalized Silicone Nanofilaments: A Novel Material for Selective Protein Enrichment. Langmuir. 2007

[17]. Donahue, HJ.; Siedlecki, CA.; Vogler, E. Osteoblastic and Osteocytic Biology and Bone Tissue Engineering. In: Hollinger, JO.; Einhorn, TA.; Doll, B.; Sfeir, C., editors. Bone Tissue Engineering. CRC Press; Boca Raton: 2004. p. 44-54.

[18]. Lim JY, Hansen JC, Siedlecki CA, Runt J, Donahue HJ. Human foetal osteoblastic cell response to polymer-demixed nanotopographic interfaces. Journal of The Royal Society Interface 2005;2:97–108.

[19]. Oner D, McCarthy TJ. Ultrahydrophobic Surfaces. Effects of Topography Length Scales on Wettability. Langmuir 2000;165:7777–82.

[20]. Miwa M, Nakajima A, Fujishima A, Hashimoto K, Watanabe T. Effects of the Surface Roughness on Sliding Angles of Water Droplets on Superhydrophobic Surfaces. Langmuir 2000;16(13):5754–60.

[21]. Tuteja A, Choi W, Ma M, Mabry JM, Mazzella SA, Rutledge GC, et al. Designing Superoleophobic Surfaces. Science December 7;2007 318(5856):1618–22. [PubMed: 18063796]2007

[22]. Zhao N, Lu X, Zhang X, Liu H, Tan S, Xu J. Progress in Superhydrophobic Surfaces. Progress in Chemistry 2007;19(6):860–71.

[23]. Feng XJ, Jiang L. Design and creation of superwetting/antiwetting surfaces. Advanced Materials Dec;2006 18(23):3063–78.

[24]. Quere D. Non-sticking drops. Reports on Progress in Physics Nov;2005 68(11):2495–532.

[25]. Li XM, Reinhoudt D, Crego-Calama M. What do we need for a superhydrophobic surface? A review on the recent progress in the preparation of superhydrophobic surfaces. Chemical Society Reviews 2007;36(8):1350–68. [PubMed: 17619692]

[26]. Zhai L, Berg MC, Cebeci FC, Kim Y, Milwid JM, Rubner MF, et al. Patterned Superhydrophobic Surfaces: Toward a Synthetic Mimic of the Namib Desert Beetle. Nano Lett 2006;6(6):1213–7. [PubMed: 16771582]

[27]. Feng L, Li S, Li Y, Li H, Zhang L, Zhai J, et al. Super-hydrophobic surfaces: from natural to artificial. Advanced Materials 2002;14(24):1857–60.

[28]. Ferrari M, Ravera F, Rao S, Liggieri L. Surfactant adsorption at superhydrophobic surfaces. Appl Phys Lett Jul;2006 89(5):3.

[29]. Shiu JY, Chen P. Addressable protein patterning via switchable superhydrophobic microarrays. Adv Funct Mater Oct;2007 17(15):2680–6.

[30]. Baeyer HCV. The Lotus Effect. The Sciences 2000;40(1):12–5.

[31]. Zhang J, Han Y. A Topography/Chemical Composition Gradient Polystyrene Surface: Toward the Investigation of the Relationship between Surface Wettability and Surface Structure and Chemical Composition. Langmuir. 2007

[32]. Marmur A. Super-hydrophobicity fundamentals: implications to biofouling prevention. Biofouling 2006;22(2):107–15. [PubMed: 16581675]

[33]. Jie-Rong C, Wakida T. Studies on the surface free energy and surface structure of PTFE film treated with low temperature plasma. Journal of Applied Polymer Science 1997;63(13):1733–9.

[34]. Ebnesajjad, S. Fluoroplastics, Volume 1: Non-Melt Processible Fluoroplastics. Plastics Design Library; Norwich, NY: 2000.

[35]. Hanford WE, Joyce RM. Polytetrafluoroethylene. Journal of the American Chemical Society 1946;68:2082–5.

[36]. Elbert DL, Hubbell JA. Surface Treatments of Polymers for Biocompatibility. Annual Review of Materials Science 1996;26:365–294.(1 %R doi:10.1146/annurev.ms.26.080196.002053)

[37]. Miyata T, Ootsuki N, Nakamae K, Okumura M, Kinomura K. Protein adsorption on a copolymer having pendant monosaccharide groups. Relationship between surface free energy and protein adsorption. Macromolecular Chemistry and Physics 1994;195(11):3597–607.

[38]. Horbett, T. Protein Adsorption on Biomaterials. In: Cooper, SL.; Peppas, NA.; Hoffman, AS.; Ratner, BD., editors. Biomaterials: Interfacial Phenomena and Applications. Am. Chem. Soc.; Washington D. C.: 1982. p. 234-43.

[39]. Horbett TA. Principles Underlying the Role of Adsorbed Plasma Proteins in Blood Interactions with Foreign Materials. Cardiovac Pathol 1993;2(3):137S–48S.

[40]. Horbett, TA. The Role of Adsorbed Proteins in Tissue Response to Biomaterials. In: Ratner, B.; Hoffman, A., editors. Biomaterials Science: An Introduction to Materials in Medicine. Vol. 2 ed.. Elsevier Academic Press; San Diego: 2004. p. 237-46.

[41]. Horbett, TA. Proteins: Structure, Properties, and Adsorption to Surface. In: Ratner, BD., editor. Biomaterials Science: an introduction to materials in medicine. Academic Press; San Diego: 1996. p. 133-41.

[42]. Andrade JD, Hlady V. Protein Adsorption and Materials Biocompatibility: A Tutorial Review and Suggested Mechanisms. Adv Polym Sci 1986;79:3–63.

[43]. Krishnan A, Sturgeon J, Siedlecki CA, Vogler EA. Scaled Interfacial Activity of Proteins at the Liquid-Vapor Interface. J Biomed Mat Res 2004;68A:544–57.

[44]. Vogler EA. Structure and Reactivity of Water at Biomaterial Surfaces. Adv Colloid and Interface Sci 1998;74(13):69–117. [PubMed: 9561719]

[45]. Lee S, Ruckenstein E. Adsorption of Proteins onto Polymeric Surfaces of Different Hydrophilicities - A Case Study with Bovine Serum Albumin. J Colloid and Interface Sci 1988;125(2):365–79.

[46]. Huang S, Ou C, Lai J. Surface composition and protein adsorption of polyurethane membrane. J Membrane Sci 1999;161(12):21–9.

[47]. Ainslie KM, Bachelder EM, Borkar S, Zahr AS, Sen A, Badding JV, et al. Cell adhesion on nanofibrous polytetrafluoroethylene (nPTFE). Langmuir 2007;23(2):747–54. [PubMed: 17209629]

[48]. Borkar S, Gu B, Dirmyer M, Delicado R, Sen A, Jackson BR, et al. Polytetrafluoroethylene nano/microfibers by jet blowing. Polymer 2006;47(25):8337–43.

[49]. Hussain AA, Awad R, Crooks PA, Dittert LW. Chloramine-T In Radiolabeling Techniques. 1. Kinetics And Mechanism Of The Reaction Between Chloramine-T And Amino-Acids. Anal Biochem Nov;1993 214(2):495–9. [PubMed: 8109739]

[50]. Hussain AA, Jona JA, Yamada A, Dittert LW. Chloramine-T In Radiolabeling Techniques. 2. A Nondestructive Method For Radiolabeling Biomolecules By Halogenation. Anal Biochem Jan;1995 224(1):221–6. [PubMed: 7710075]

[51]. Walker, JM. The protein protocols handbook. Vol. 2nd ed.. Humana Press; Totowa, N.J.: 2002.

[52]. Krishnan A, Siedlecki C, Vogler EA. Traube-Rule Interpretation of Protein Adsorption to the Liquid-Vapor Interface. Langmuir 2003;19:10342–52.

[53]. Krishnan A, Wilson A, Sturgeon J, Siedlecki CA, Vogler EA. Liquid-Vapor Interfacial Tension of Blood Plasma, Serum and Purified Protein Constituents Thereof. Biomaterials 2005;26:3445–53. [PubMed: 15621233]

[54]. Krishnan A, Liu Y-H, Cha P, Allara DL, Vogler EA. Interfacial Energetics of Globular-Blood Protein Adsorption to a Hydrophobic Surface from Aqueous-Buffer Solution. Journal of the Royal Society Interface 2006;3:283–301.

[55]. Krishnan A, Liu Y-H, Cha P, Allara DL, Vogler EA. Scaled Interfacial Activity of Proteins at a Hydrophobic Solid/Aqueous-Buffer Interface. J Biomed Mater Res 2005;75A(2):445–57.

[56]. Krishnan A, Liu Y-H, Cha P, Allara DL, Vogler EA. Interfacial Energetics of Blood Plasma and Serum Adsorption to a Hydrophobic Self-Assembled Monolayer Surface. Biomaterials 2006;27:3187–94. [PubMed: 16494939]

[57]. Ariola F, Krishnan A, Vogler EA. Interfacial Rheology of Blood Proteins Adsorbed to the Aqueous-Buffer/Air Interface. Biomaterials 2006;27:3404–12. [PubMed: 16504286]

[58]. Cha P, Krishnan A, Fiore VF, Vogler EA. Interfacial Energetics of Protein Adsorption from Aqueous Buffer to Surfaces with Varying Hydrophilicity. Lagmuir. 2007in press

[59]. Barnthip N, Noh H, Leibner E, Vogler EA. Volumetric Interpretation of Protein Adsorption: Kinetic Consequences of a Slowly-Concentrating Interphase. Biomaterials 2008;29:3062–74. [PubMed: 18442850]

[60]. Noh H, Vogler EA. Volumetric Interpretation of Protein Adsorption: Partition Coefficients, Interphase Volumes, and Free Energies of Adsorption to Hydrophobic Surfaces. Biomaterials 2006;27:5780–93. [PubMed: 16919724]

[61]. Noh H, Vogler EA. Volumetric Interpretation of Protein Adsorption: Mass and Energy Balance for Albumin Adsorption to Particulate Adsorbents with Incrementally-Increasing Hydrophilicity. Biomaterials 2006;27:5801–12. [PubMed: 16928398]

[62]. Noh H, Vogler EA. Volumetric Interpretation of Protein Adsorption: Competition from Mixtures and the Vroman Effect. Biomaterials 2007;28:405–22. [PubMed: 17007920]

[63]. Noh H, Vogler EA. Volumetric Interpretation of Protein Adsorption: Ion-Exchange Adsorbent Capacity, Protein pI, and Interaction Energetics. Biomaterials. 2006in press

[64]. Krishnan A, Siedlecki CA, Vogler EA. Mixology of Protein Solutions and the Vroman Effect. Langmuir 2004;20(12):5071–8. [PubMed: 15984270]

[65]. Helfrich JP. Flow-Mode Dynamic Laser Light Scattering Technology for 21st Century Biomolecular Characterization. Am Biothech Lab 1998;16(11):64–6.

[66]. Ainslie KM, Sharma G, Dyer MA, Grimes CA, Pishko MV. Attenuation of protein adsorption on static and oscillating magnetostrictive nanowires. Nano Lett Sep;2005 5(9):1852–6. [PubMed: 16159237]

[67]. Du YJ, Cornelius RM, Brash JL. Measurement of protein adsorption to gold surface by radioiodination methods: suppression of free iodide sorption. Colloid Surf B-Biointerfaces Jan;2000 17(1):59–67.

[68]. Goncalves IC, Martins MCL, Barbosa MA, Ratner BD. Protein adsorption on 18-alkyl chains immobilized on hydroxyl-terminated self-assembled monolayers. Biomaterials Jun;2005 26(18): 3891–9. [PubMed: 15773038]

[69]. Paynter RW, Ratner BD, Horbett TA, Thomas HR. XPS Studies On The Organization Of Adsorbed Protein Films On Fluoropolymers. J Colloid Interface Sci 1984;101(1):233–45.

[70]. Sheardown H, Cornelius RM, Brash JL. Measurement of protein adsorption to metals using radioiodination methods: a caveat. Colloid Surf B-Biointerfaces Oct;1997 10(1):29–33.

[71]. Stahl JB, Debe MK, Coleman PL. Enhanced bioadsorption characteristics of a uniquely nanostructured thin film. J Vac Sci Technol A-Vac Surf Films May-Jun;1996 14(3):1761–5.

[72]. Uyen HMW, Schakenraad JM, Sjollema J, Noordmans J, Jongebloed WL, Stokroos I, et al. Amount And Surface-Structure Of Albumin Adsorbed To Solid Substrata With Different Wettabilities In A Parallel Plate Flow Cell. J Biomed Mater Res Dec;1990 24(12):1599–614. [PubMed: 2277056]

[73]. Wei J, Helm GS, Hou XL. Quantification of protein adsorption on membrane surfaces by radiolabeling technique. Desalination Nov;2006 199(13):378–80.

[74]. Anraku M, Kragh-Hansen U, Kawai K, Maruyama T, Yamasaki Y, Takakura Y, et al. Validation of the chloramine-T induced oxidation of human serum albumin as a model for oxidative damage in vivo. Pharm Res Apr;2003 20(4):684–92. [PubMed: 12739779]

[75]. Desbuquo B, Aurbach GD. Effects of Iodination on Distribution of Peptide Hormones in Aqueous 2-Phase Polymer Systems. Biochemical Journal 1974;143(1):83–91. [PubMed: 4464859]

[76]. Efimova YM, Wierczinski B, Haemers S, van Well AA. Changes in the seconary structure of proteins labeled with I-125: CD spectroscopy and enzymatic activity studies. J Radioanal Nucl Chem Apr;2005 264(1):91–6.

[77]. Holmberg M, Stibius KB, Ndoni S, Larsen NB, Kingshott P, Hou XLL. Protein aggregation and degradation during iodine labeling and its consequences for protein adsorption to biomaterials. Anal Biochem Feb;2007 361(1):120–5. [PubMed: 17187752]

[78]. Osborne JC, Schaefer EJ, Powell GM, Lee NS, Zech LA. Molecular-Properties Of Radioiodinated Apolipoprotein-A-I. J Biol Chem 1984;259(1):347–53. [PubMed: 6423628]

[79]. Hunter JR, Kilpatrick PK, Carbonell RG. Lysozyme Adsortion at the Air/Water Interface. J Colloid and Interface Sci 1989;137(2):462–82.

[80]. Minghetti PP, Ruffner DE, Kuang WJ, Dennison OE, Hawkins JW, Beattie WG, et al. Molecular-Structure Of The Human-Albumin Gene Is Revealed By Nucleotide-Sequence Within Q11-22 Of Chromosome-4. J Biol Chem 1986;261(15):6747–57. [PubMed: 3009475]

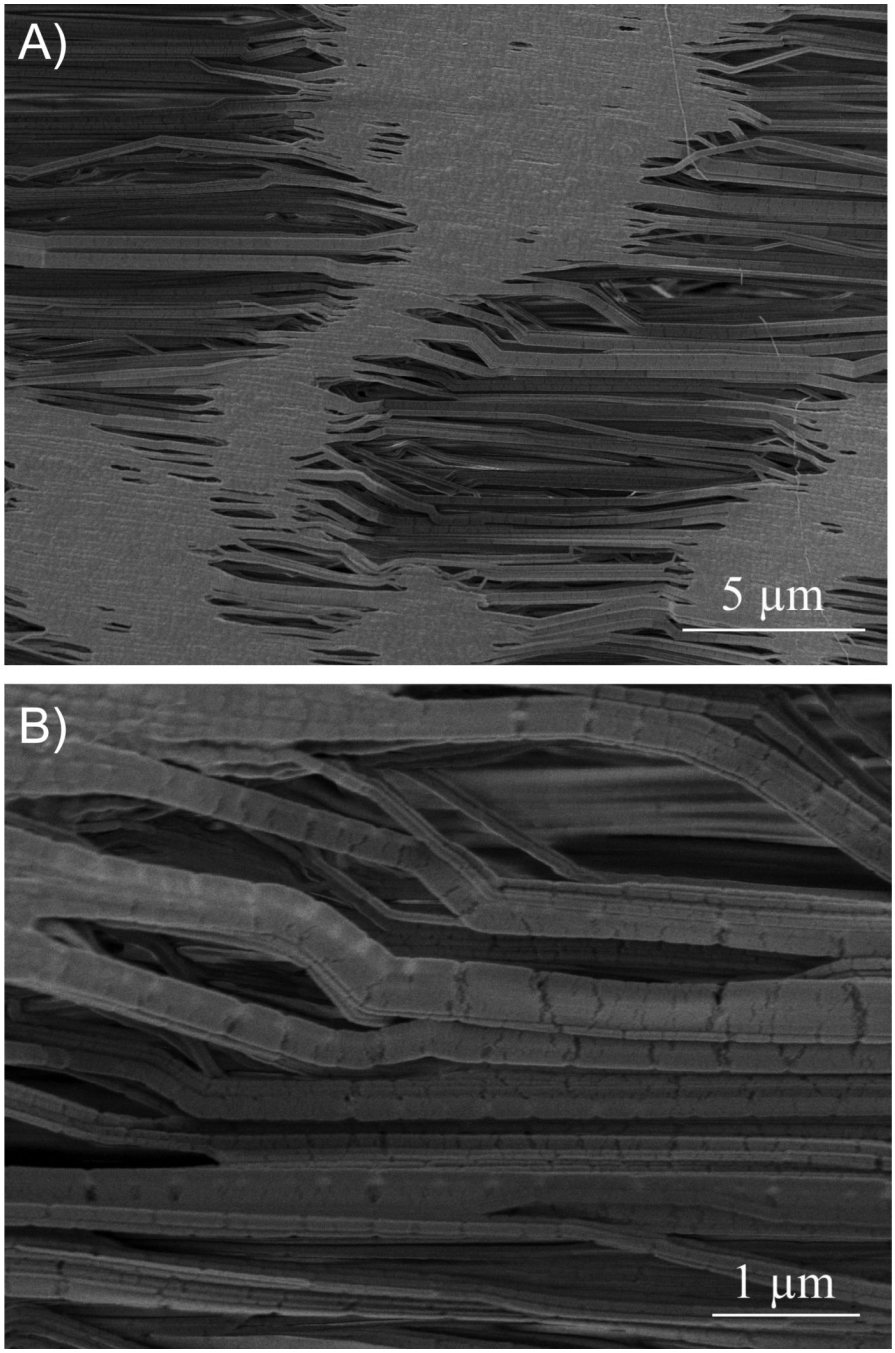

Figure 1.
Field Emission Scanning Electron Microscopy (FESEM) images of ePTFE at 5,000X (Panel A) and 20,000X (Panel B) showing fibular structure of the expanded PTFE matrix. ePTFE exhibits superhydrophobic wetting properties with water contact angles in excess of 150°.

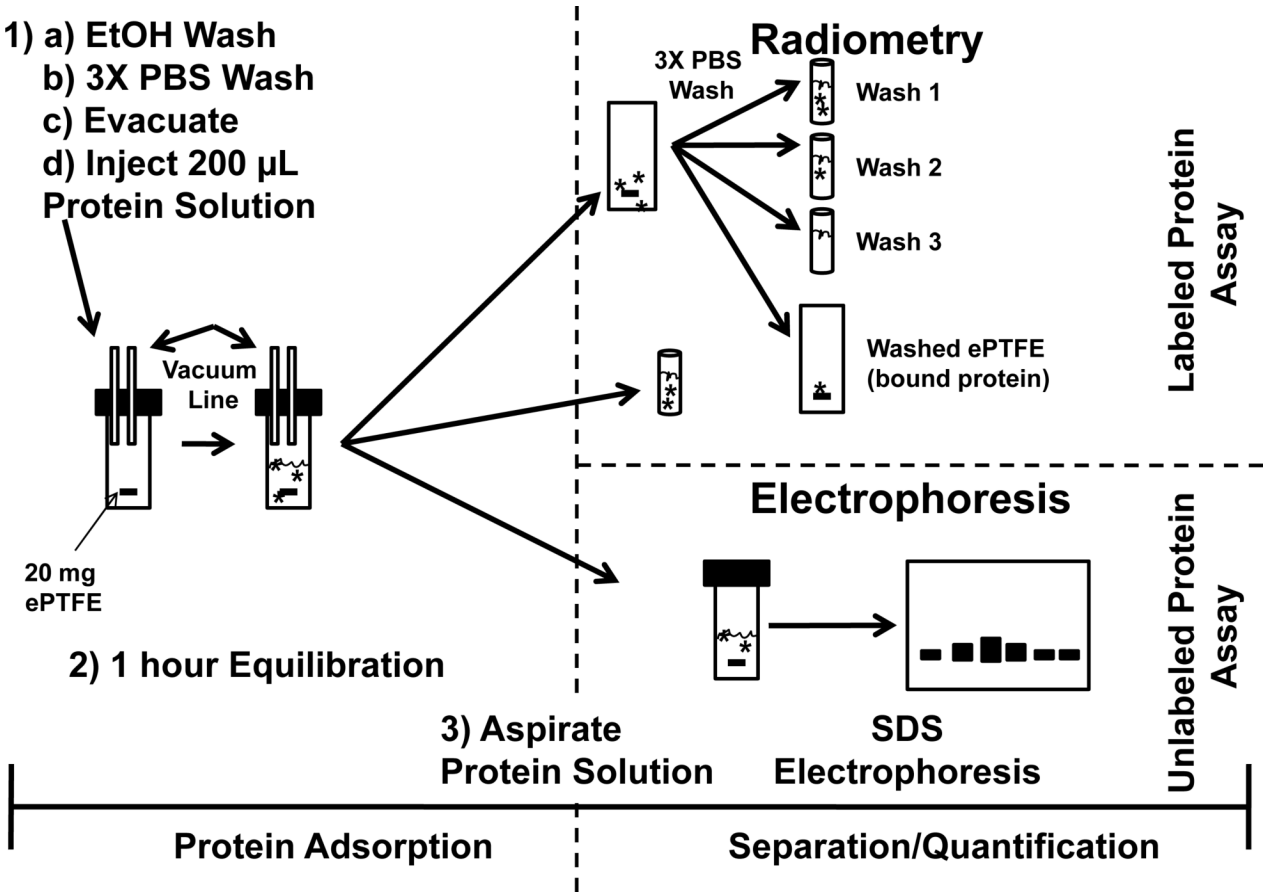

Figure 2.

Experimental flow chart outlining the procedures used to measure HSA adsorption to superhydrophobic ePTFE using either radiometry or electrophoresis as methods of protein quantification. Left-hand side illustrates critical steps of air removal and pre-wetting that assures intimate contact of the fibular ePTFE structure with protein solution. Protein molecules (*, with radiolabel for radiometry and without radiolabel for electrophoresis) adsorb to ePTFE and are distributed between surface and solution at steady state (1 hour). Solution depletion is quantified by either radiometry (upper left panel) or by electrophoresis (lower left panel, see Section 2). Radiolabeled HSA bound to ePTFE was measured after 3X serial rinse of adsorbent with PBS.

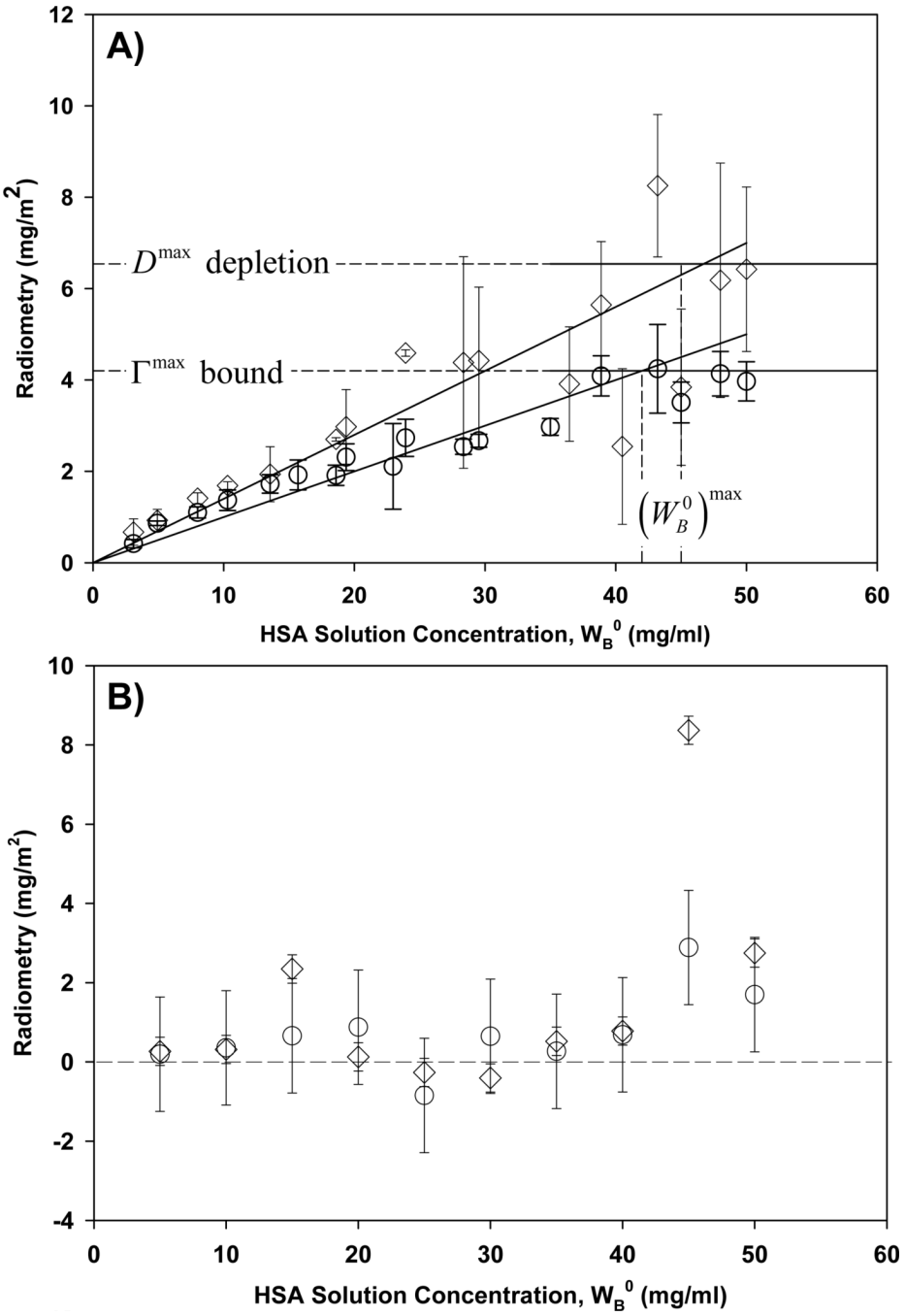

Figure 3.

Radiometric adsorption isotherms measured with (Panel A) and without (Panel B) solution degassing and removal of air from ePTFE adsorbent (see Figure 5), comparing amounts of HSA bound to the surface (open circles) to the amount depleted from solution (diamonds). Nearly no adsorbed HSA was measured without removal of air and results were erratic at higher solution concentrations. Error bars represent mean and standard deviation of triplicate trials at each solution concentration. Lines through the data of Panel A represent statistical treatment of isotherm data as described in Section 2 that identify the maximal amount of protein adsorbed

Γ^{max} (bound HSA) and D^{max} (depletion) that occurs at the solution concentration $\left(W_B^o\right)^{max}$ indicated by horizontal line annotations.

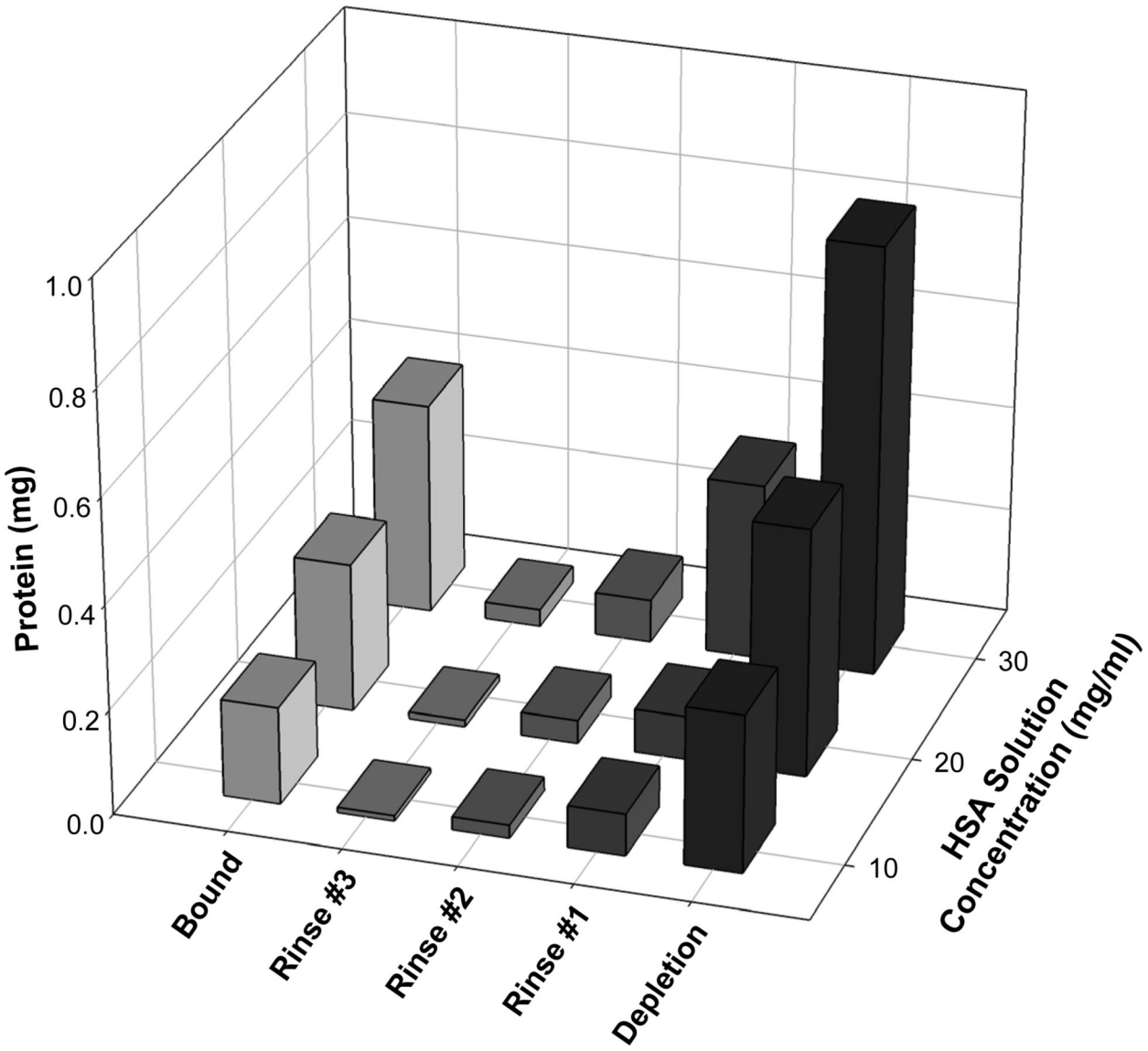

Figure 4.

Distribution of radiolabeled HSA in a single adsorption trial at three different solution concentrations (see Figure 5). The total amount of HSA adsorbed measured by depletion was greater than the amount remaining (bound fraction) after 3X serial PBS rinses of the ePTFE adsorbent. Third rinse contained negligible quantities of HSA.

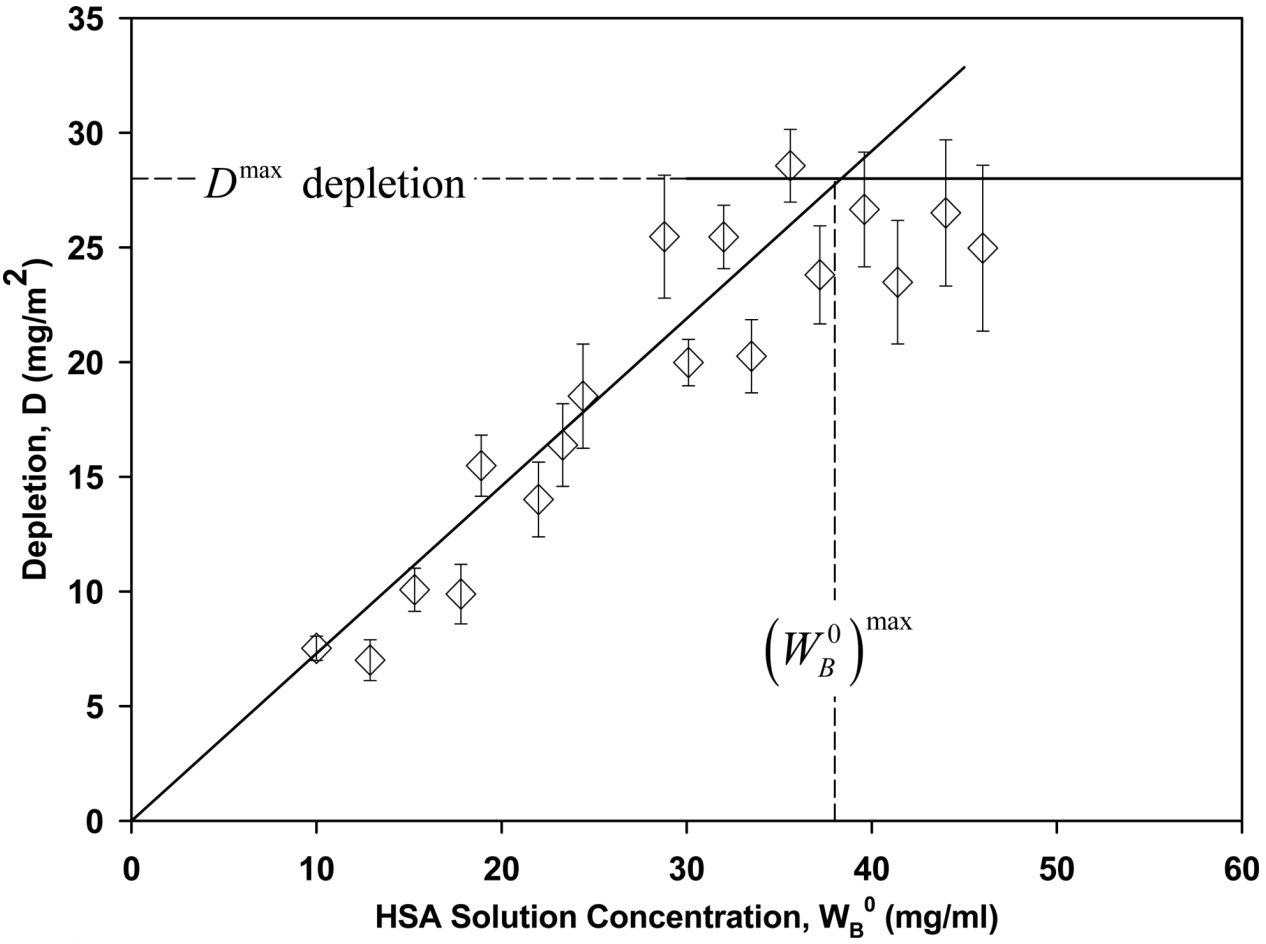

Figure 5.

HSA adsorption to ePTFE measured by solution depletion quantified by electrophoresis. Lines through the data represent statistical treatment of isotherm data as described in Section 2 that identifies the maximal amount of protein adsorbed D^{max} that occurs at the solution concentration $\left(W_B^o\right)^{max}$ indicated by the horizontal line annotation. Comparison to depletion results of Figure 2A shows that the more unlabelled HSA adsorbs to the same surface area of ePTFE than labeled HSA.

Table 1

Characteristic HSA Adsorption Parameters by Radiometry and Depletion

Radiometry				
Adsorbed Fraction	D^{max} **(unit)** **(N, Std. Dev.)**	Γ^{max} **(*unit*)** **(N, Std. Dev.)**	***S* (*unit*)** **(*N*, R^2)***	$\left(W_B^0\right)^{max}$**(*unit*)**
Bound	-	4.20±0.59 (mg/m^2) (18,0.92)	0.10±0.005 (mL/m^2) (11,0.81)	42.39±6.32 (mg/mL)
Total	3.73±1.77(mg/mL) (17,0.70)	-	0.08±0.005 (11,0.84)	46.16±22.07 (mg/mL)
	6.54±2.60 (mg/m^2) (17,0.70)	-	0.14±0.009 (mL/m^2) (13,0.84)	45.24±18.17 (mg/mL)
Electrophoresis				
Total	15.97±1.73 (mg/mL) (18,0.89)	-	0.41±0.022 (9,0.84)	38.74±4.67 (mg/mL)
	28.46±3.08 (mg/m^2) (18,0.89)	-	0.73±0.039 (mL/m^2) (9,0.84)	38.75±4.67 (mg/mL)

Notes: Bound = protein remaining after 3X PBS rinse. Total = protein depleted from solution.

*(*N*, R^2) = (number of data points, R^2 of linear regression through the adsorption isotherm)